DOI 10.1007/s10527-020-09993-3
Biomedical Engineering, Vol. 54, No. 2, July, 2020, pp. 149-154. Translated from Meditsinskaya Tekhnika, Vol. 54, No. 2, Mar.-Apr., 2020, pp. 51-55.
Original article submitted December 16, 2019.

3D Ultrasound: Visualization of Volumetric Data

L. V. Osipov[1], N. S. Kulberg[1], D. V. Leonov[1,2]*, and S. P. Morozov[1]

This article continues a previously published review, "3D ultrasound: Current state, emerging trends and technologies," which was the first part in a cycle addressing 3D/4D ultrasound technologies. The first part explained the basic mechanisms for obtaining three-dimensional ultrasound images and considered the physical basis, advantages, and drawbacks associated with the use of transducers and the main methods of volumetric scanning. The present article describes the capabilities of the state-of-the-art diagnostic ultrasound scanners to visualize 3D/4D data.

Introduction

The result of volumetric scanning using any of the methods described in [1] is that a three-dimensional dataset is formed in the memory of an ultrasound device, i.e., an image of the region of interest. However, to facilitate the reading for sonographers the data must be iteratively converted and displayed on a screen. *The goal of the present article* is to outline the main features of the three-dimensional visualization available to the users of state-of-the-art diagnostic ultrasound instruments.

Preparatory Measures

Before discussing the visualization methods, we need to address some of the accessory operations that give meaning to the scanned images.

During the volumetric scanning, digitized echoes form a three-dimensional set of numbers, each of which corresponds to some point in the region of interest. Figure 1a shows a scheme for obtaining a sample image using the convex mechanical method (mechanical scanning plane 2 is rotated by 90° for convenience). If the scan data are displayed on the screen as it is, the image will be strongly distorted (Fig. 1b). We can see that the objects located closer to the probe are stretched horizontally and the straight lines become curved. This comes from the fact that the datasets, consisting of traces of individual "beams," are formed in different and sometimes very exotic curvilinear coordinate systems. Therefore, converting the datasets to the Cartesian coordinate system familiar to the user (i.e., *scan conversion* [1, 2]) is essential. Interpolation fills the "voids" between the diverging beams formed in the scan conversion process.

Figure 1b shows image brightness distortion: of the many objects studied, only the brightest can be distinguished by the observer. This is due to the physical reflectance properties of the environment: bright objects (for example, vessel walls, tendons) reflect ultrasound hundreds of times more intensely than diffuse reflective objects (such as the liver parenchyma and the kidneys). To make these objects distinguishable from each other's backgrounds, the brightness range is logarithmically compressed.

All the actions listed above are common to the visualization of two- and three-dimensional ultrasound. However, the structure of the three-dimensional dataset presents a significantly more complex computational task, as is illustrated by a simple calculation. The typical amount of memory needed for a two-dimensional B-mode image in a standard scanner is defined by a matrix of 512 × 512 pixels with 256 grayscale gradations. The volume of data for the three-dimensional image increases by no fewer than the factor corresponding to the number

[1] Research and Practical Clinical Center for Diagnostics and Telemedicine Technologies of the Moscow Healthcare Department, Moscow, Russia; E-mail: d.leonov@npcmr.ru
[2] National Research University "Moscow Power Engineering Institute", Moscow, Russia.
* To whom correspondence should be addressed.

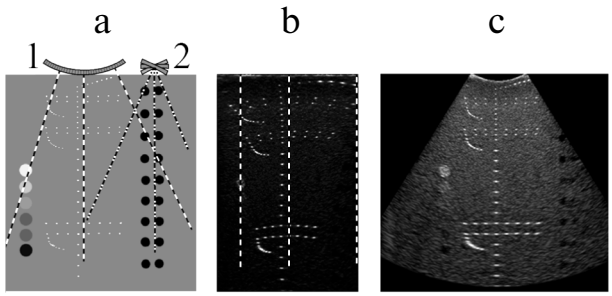

Fig. 1. Transformation of coordinates in convex mechanical scanning: a) diagram of reflections in a tissue-equivalent phantom and ray acquisition order in the electronic (1) and mechanical (2) scanning directions; dashed lines show possible ray directions; b) example of a "raw image" without transformation of coordinates to the electronic scanning coordinate and without compression of the brightness range; c) image after transformation of coordinates.

of image slices obtained (for example, 64). This imposes strict requirements on the manufacturers of the three-dimensional visualization systems, which in turn increases their cost.

The Main Problems in Visualizing 3D Data

Human vision is fundamentally unable to perceive complete volumetric information. The "volumetric" images we are familiar with are formed by pairs of flat pictures formed on the retinas. We see most of the objects as the two-dimensional surfaces of three-dimensional objects. The so-called volumetric stereoscopic vision allows us to assess distances to objects but does not allow us, for example, to see one object behind the other. When the human eye observes real volumetric data (for example, superimposition of semitransparent objects), the background image is often misinterpreted.

This confronts investigators with the task of "simplifying" the three-dimensional dataset to such a state that a human can perceive it without effort. This is done using different approaches to representing three-dimensional images on a flat screen. We will consider the main methods in detail.

Pseudo Volumetric Representation

This method relies on the mean values closest to the natural means of volumetric vision in humans. Special algorithms allow extraction of object surfaces in three-dimensional datasets when the acoustic characteristics of the objects are notably different from those of the adjacent structures and tissues. This leads to the construction of a *pseudo volumetric image of surfaces*. For example, in obstetrics, where the development of 3D ultrasound scan methods started more than three decades ago [3], the pseudo volumetric representation can produce images of the external surfaces of the fetus (Fig. 2a). Such images allow the clinician to assess developmental anomalies of the fetal face and body [4, 5]. Noise suppression and smoothing are widely used to improve visualization quality [6, 7].

Three-dimensional information is generally shown on monitors as two-dimensional images, so the investigator has to be content with planar images of the volumetric object. Approaches widely employed in the visual arts apply in this case to medicine. The software applies pseudo shadowing to emphasize the three-dimensional image details to a flat image as though surface relief is highlighted from a particular angle. This technique is called *rendering* [8]. The orientation of the surface can be changed by rotating the object. This method is mostly used in obstetrics and perinatology for imaging of the fetus (Fig. 2, a-c) [9].

Another technique used to present 3D data on a flat screen in a meaningful way is called *depth colorization*

Fig. 2. Pseudo volumetric and semitransparent visualization: a) fetal face [17]; b) fetus at week 14 [18]; c) the ulna and radius of a fetus; d) surface of the mitral valve [10, 19]; e, f) vessels in Doppler energy mode; g, h) semitransparent representations: fetal skeleton (g) and body (h).

(Fig. 2d). Depth colorization assigns a color to each pixel depending on its depth. Parts of the surface located close to the probe are highlighted with lighter tones, such as yellow. Deeper areas are shown in darker colors, sometimes with a gradual transition to light and dark blues. In echocardiography, depth colorization helps to visualize the movement of the heart valves [6, 10, 11].

Studies of the vascular bed and blood flow utilize reconstructed three-dimensional images of vessels (Fig. 2, e and f). Vessels are differentiated based on the presence of blood flow [12-14]. The preparation of three-dimensional images of vessels using Doppler modes always involves a significant reduction in frame rate.

Toshiba (Japan) has developed a new technology called virtual endoscopy (*Fly Thru©)*. It visualizes the inner surfaces of hollow organs and vessels as though they were observed from the inside [15, 16].

Semitransparent Representation

The *semitransparent representation* makes some objects or structures seen through the others (Fig. 2, g and h). Examples of the modes for semitransparent representation of superficial soft tissues and bony structures are *X-ray transparency mode*, *maximum transparency mode, crystal view*, etc. Studies have shown that these modes give more complete information about the development of fetal bony structures and ensure better evaluation of their outlines, thickness, and mineralization compared to the standard 2D ultrasound investigation [21, 22].

Slice-by-Slice Display

The images obtained by these modes resemble the B scans obtained by conventional two-dimensional ultrasound scanning. This may give a false impression that this method is a "step backward" compared to the pseudo volumetric and semitransparent modes, though this is far from true.

The screen representation mode based on *multiple arbitrarily oriented slices* of a volumetric object allows the clinician to single out and use the most informative slice for analysis (Fig. 3, a-c) [23]. Figure 3c shows an example of a slice-by-slice mammogram. The transverse slices presented here clearly show a hypoechogenic area and an acoustic shadow, which is indicative of a potentially dangerous neoplasm.

Another mode called *multi-slice view* shows multiple slices of tomographic images, mostly of uniform thickness [24-26]. In perinatology, for example, the examination of a series of slices of the nuchal fold of the fetus allows measuring the fetal size with greater accuracy (Fig. 3d) [18].

Significant advantages of the slice-by-slice representation over standard two-dimensional scanning come from the ability to select the required slice on retrospective analysis when data collection has already been completed and projections inaccessible to standard two-dimensional scanning can be obtained. The slice-by-slice representation is preferable when a doctor needs to analyze particular slices instead of looking at a complete volume as in the pseudo volumetric representation. Isometric representation of a three-dimensional object with the ability to make cutouts using the main sections at different depths or levels combines the convenience of the pseudo volumetric visualization and the accuracy of the slice-by-slice representation (Fig. 3e).

Real-Time Doppler Modes

Obtaining a 4D dataset by Doppler color mapping is associated with major difficulties since it is both intensively resource- and time-consuming. However, for small objects, such as the fetal heart or individual heart valves, the *color STIC* mode gives useful diagnostic information

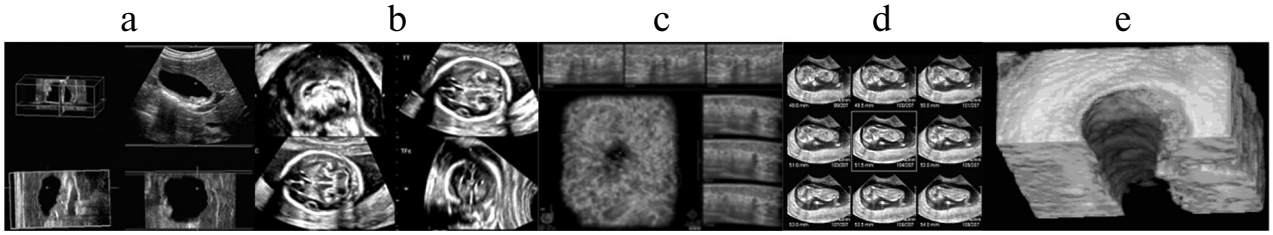

Fig. 3. Slice-by-slice representation: a) gallbladder [20]; b) fetal brain [18]; c) breast [27]; d) combined two-dimensional slices and pseudo volumetric reconstruction; e) vessel lumen [18].

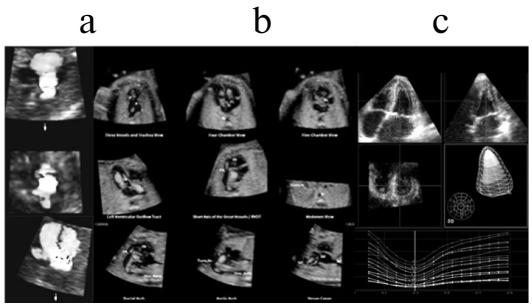

Fig. 4. Real-time imaging of the heart: a) three slices using color STIC [18]; b) blood flow in nine standard planes [29]; c) segmentation of the left ventricle and a plot showing how the segment cross-sections change in size over time.

[28]. By rotating, the dynamic 3D map of blood flow can be examined from different points of view. Figure 4a shows three slices of the fetal heart obtained in *real-time 4D* mode using color Doppler blood flow mapping. These images show clear signs of mitral valve failure. The color STIC mode uses blood flow mapping to study fetal cardiac hemodynamics and assess developmental anomalies [18].

A new mode was recently developed which analyses 3D echocardiograms and automatically displays nine standard cardio planes with superimposed dynamic map of blood flow [29, 30]. The mode is called *5D Fetal Heart Color* [31-34]. It starts with four-dimensional STIC data. The operator sequentially marks orientation points on the display and then the software automatically shows the fetal heart in the nine standard planes (Fig. 4b).

Today the three-dimensional echocardiography investigations find ever wider use as the method provides better diagnostic capabilities [35]. One of the techniques is based on the processing of 3D/4D data to obtain quantitative measurements of the heart function, especially the left ventricle [1, 23]. This task involves a special type of representation of the heart chambers and a diagnostic mode for representing the heart operation diagrams (Fig. 4c).

Conclusions

3D/4D ultrasound visualization has always drawn the attention of researchers and medical device developers. However, despite the growing interest, many key questions remain unanswered, which is why the volumetric ultrasound scan technologies to this day have not become an obligatory tool in many branches of medicine. It is still widely believed that these technologies do not provide new diagnostic data to experienced clinicians who operate very effectively with 2D ultrasound scans. At the same time, these technologies have attracted significant attention from patients (for example, pregnant women), as volumetric images are dazzling and easy to interpret.

The ease of interpreting the 3D/4D ultrasound scan data (particularly *stereoscopic representation* of anatomical structures) makes these technologies a perfect tool for medical training [36, 37]. It is known that, unlike MRI and CT images, reading two-dimensional ultrasound images is especially challenging for trainees. The use of three-dimensional technologies in training will make it easier for the trainees to understand the principles of ultrasound imaging.

Ultrasound is used during surgery to dynamically assess organs and tissues being operated [38]. CT or MRI maps of the planned incisions made before the surgery are compared with ultrasound images obtained during the procedure. Real-time monitoring is vital, as organs can be displaced and deformed. 2D ultrasound scanning serves as the standard for real-time surgical monitoring. There are studies describing a similar mode of 3D ultrasound scanning, but the potential of such investigations remains to be unraveled [39-42].

Another potential area of focus involves diagnostics of mineral inclusions such as kidney stones, microcalcifications of the breast, and other objects, whose density makes it possible to distinguish them from surrounding tissues [43-47]. The use of volumetric representations allows 3D ultrasound scanning to produce both additional information on the morphology of individual mineral inclusions and to improve the assessment of the accumulation shapes.

One of the barriers to the wider use of 3D/4D ultrasound scanning is the variety of user interfaces and large differences in the control element layout between the manufacturers. A common approach to interface design will alleviate the need for specialist retraining.

This work was supported by the Russian Foundation for Basic Research (Grant No. 17-01-00601).

REFERENCES

1. Osipov, L. V., Kulberg, N. S., Leonov, D. V., and Morozov, S. P., "3D ultrasound: Current state, emerging trends and technologies," Biomed. Eng., **52**, No. 3, 199-203 (2018).
2. Osipov, L. V., Ultrasound Diagnostic Devices: Modes, Methods, and Technologies [in Russian], Izomed, Moscow (2011).
3. Baba, K., Satoh, K., Sakamoto, S., Okai, T., and Ishii, S., "Development of an ultrasonic system for three-dimensional

reconstruction of the fetus," J. Perinat. Med., **17**, No. 1, 19-24 (1989).
4. Werner, H., Marcondes, M., Daltro, P., Fazecas, T., Ribeiro, B. G., Nogueira, R., and Araujo Júnior, E., "Three-dimensional reconstruction of fetal abnormalities using ultrasonography and magnetic resonance imaging," J. Matern. Fetal Neonatal Med. (2018); https://doi.org/10.1080/14767058.2018.1465558 (accessed March 15, 2019).
5. Dall'Asta, A., Schievano, S., Bruse, J. L., Paramasivam, G., Kaihura, C. T., Dunaway, D., and Lees, C. C., "Quantitative analysis of fetal facial morphology using 3D ultrasound and statistical shape modeling: A feasibility study," Am. J. Obstet. Gynecol., **217**, No. 1, 76.e1-76.e8 (2017).
6. Birkeland, E., Solteszova, V., Hönigmann, D., Gilja, O. H., Brekke, S., Ropinski, T., and Viola, I., "The ultrasound visualization pipeline – A survey," ArXiv e-prints; arXiv: 1206.3975 (2012) (accessed March 15, 2019).
7. Kulberg, N. S., Yakovleva, T. V., Kamalov, Yu. R., Sandrikov, V. A., Osipov, L. V., and Belov, P. A., "Development and trial of a new method of image enhancement for ultrasonic medical diagnostics," Acoust. Phys., **55**, No. 4-5, 538-546 (2009).
8. Huang, Q. and Zeng, Z., "A Review on real-time 3D ultrasound imaging technology," BioMed Res. Int., Article ID 6027029 (2017).
9. Singh, K. and Malhotra, N., Step by Step: 3D/4D Ultrasound in Obstetrics, Gynecology and Infertility, Jaypee Brothers Medical Publishers (2013), 2nd Edition.
10. Takahiro, S., "Role of modern 3D echocardiography in valvular heart disease," Korean J. Intern. Med., **29**, No. 6, 685-702 (2014).
11. Takahiro, S., "3D echocardiography: the present and the future," J. Cardiol., **52**, No. 3 169-185 (2008).
12. Nasnikova, I. Yu. and Kharlap, S. I., "Ultrasound volumetric spatial visualization and the potential for its use in ophthalmology," Med. Vizual., No. 3, 49-58 (2003).
13. Pelz, J. O., Weinreich, A., Karlas, T., and Saur, D., "Evaluation of freehand B-mode and power-mode 3D ultrasound for visualisation and grading of internal carotid artery stenosis," PLoS One, **12**, No. 1, 1-11 (2017).
14. Caresio, C., Caballo, M., Deandrea, M., Garberoglio, R., Mormile, A., Rossetto, R., Limone, P., and Molinari, F., "Quantitative analysis of thyroid tumors vascularity: A comparison between 3-D contrast-enhanced ultrasound and 3-D Power Doppler on benign and malignant thyroid nodules," Med. Phys., **45**, No. 7, 3173-3184 (2018).
15. Grant, E. G., "Advanced techniques in 4D ultrasound: Fly Thru," Toshiba, ULWP12028US [online resource], http://www.mttechnica.ru/UserFiles/File/Whit_Pap_Fly_Thru_11_2012_MWPUL0019RUC_Final_NEWSIZE.pdf (accessed March 15, 2019).
16. Tesarik, J., Mendoza-Tesarik, R., and Mendozaet, N., "Virtual sonographic embryoscopy: A new tool for evaluation of early pregnancy," EC Gynaecology, **5**, No. 2, 69-71 (2017).
17. Mindray [online resource], http://mindrayultrasound.net (accessed March 15, 2019).
18. Samsung Medison [online resource], https://www.samsungmedison.com (accessed March 15, 2019).
19. Philips [online resource], https://www.philips.ru/healthcare (accessed March 15, 2019).
20. GE Healthcare [online resource], https://www.gehealthcare.com (accessed March 15, 2019).
21. Achiron, R., Gindes, L., Zalel, Y., Lipitz, S., and Weisz, B., "Three- and four-dimensional ultrasound: New methods for evaluating fetal thoracic anomalies," Ultrasound Obstet. Gynecol., **32**, No. 1 36-43 (2008).
22. Dall'Asta, A., Paramasivam, G., and Lees, C. C., "Crystal Vue technique for imaging fetal spine and ribs," Ultrasound Obstet. Gynecol., **47**, No. 3, 383-384 (2016).
23. Simpson, J. M. and Miller, O., "Three-dimensional echocardiography in congenital heart disease," Arch. Cardiovasc. Dis., **104**, 45-56 (2011).
24. Alcazar, J. L., Pascual, M. A., Ajossa, S., de Lorenzo, C., Piras, A., Hereter, L., Juez, L., Fabbri, P., Graupera, B., and Guerriero, S., "Reproducibility of the International Endometrial Analysis Group Color Score for assigning the amount of flow within the endometrium using stored 3-dimensional volumes," J. Ultrasound Med., No. 36, 1347-1354 (2017).
25. Cariello, L., Montaguti, E., Cataneo, I., Dodaro, G., Margarito, E., Rizzo, N., and Youssef, A., "The levator–urethral gap measurement: Tomographic ultrasound imaging (TUI) versus Omniview-volume contrast imaging (VCI)," Ultrasound Obstet. Gynecol., **50**, Supplement 1, 141 (2017).
26. Fukuda, H., Numata, K., Hara, K., Nozaki, A., Kondo, M., Chuma, M., Nakano, M., Nozawa, A., Maeda, S., and Tanaka, K., "Comparison of vascularity observed using contrast-enhanced 3D ultrasonography and pathological changes in patients with hepatocellular carcinoma after sorafenib treatment," J. Cancer, **9**, No. 13, 2408-2414 (2018).
27. Shin, H. J., Kim, H. H., and Cha, J. H., "Current status of automated breast ultrasonography," Ultrasonography, **34**, No. 3, 165-172 (2015).
28. Araujo, E., Tonni, G., Bravo-Valenzuela, N. J., Da Silva Costa, F., and Meagher, S., "Assessment of fetal congenital heart diseases by 4-dimensional ultrasound using spatiotemporal image correlation: pictorial review," Ultrasound Q., **34**, No. 1, 11-17 (2018).
29. Yeo, L. and Romero, R., "Fetal intelligent navigation echocardiography (FINE): A novel method for rapid, simple, and automatic examination of the fetal heart," Ultrasound Obstet. Gynecol., **42**, No. 3, 268-284 (2013).
30. Dall'Asta, A., Paramasivam, G., and Lees, C. C., "Qualitative evaluation of Crystal Vue rendering technology in assessment of fetal lip and palate," Ultrasound Obstet. Gynecol., **49**, No. 4, 549-552 (2017).
31. "5D Heart Color: automatic examination of the fetal heart based on intelligent navigation technology," Samsung Medison, Article ID CL201510-5DHeartColor (2015).
32. Yeo, L., Luewan, S., and Romero, R., "Fetal intelligent navigation echocardiography (FINE) detects 98% of congenital heart disease," J. Ultrasound Med., **37**, No. 11, 2577-2593 (2018).
33. Yeo, L. and Romero, R., "Color and power Doppler combined with Fetal Intelligent Navigation Echocardiography (FINE) to evaluate the fetal heart," Ultrasound Obstet. Gynecol., **50**, No. 4, 476-491 (2017).
34. Veronese, P., Bogana, G., Cerutti, A., Yeo, L., Romero, R., and Gervasi, M. T., "A prospective study of the use of Fetal Intelligent Navigation Echocardiography (FINE) to obtain standard fetal echocardiography views," Fetal Diagn. Ther., **41**, No. 2, 89-99 (2017).
35. Kozlowski, P., Urheimz, S., and Samset, E., "Evaluation of a multi-view autostereoscopic real-time 3D ultrasound system for minimally invasive cardiac surgery guidance," IEEE 14th International Symposium on Biomedical Imaging (2017), pp. 604-607.
36. Remmele, M., Schmidt, E., Lingenfelder, M., and Martens, A., "The impact of stereoscopic imagery and motion on anatomical structure recognition and visual attention performance," Anat. Sci. Educ., **11**, No. 1 15-24 (2017).
37. Hackett, M. and Proctor, M., "Three-dimensional display technologies for anatomical education: A literature review," J. Sc. Educ. Technol., No. 25, 641-654 (2016).
38. Leonov, D. V., Fin, V. A., and Gukasov, V. M., "The current state and trends in the development of ultrasound medical diagnostic devices," Med. Vys. Tekhnol., No. 3, 8-13 (2014).

39. Lange, T., Papenberg, N., Heldmann, S., Modersitzki, J., Fischer, B., Lamecker, H., and Schlag, P. M., "3D ultrasound-CT registration of the liver using combined landmark-intensity information," Int. J. Comput. Assist. Radiol. Surg., **4**, No. 1, 79-88 (2009).
40. Simpson, A. L. and Kingham, T. P., "Current evidence in image-guided liver surgery," J. Gastrointest. Surg., **20**, No. 6, 1265-1269 (2016).
41. Clements, L. W., Collins, J. A., Weis, J. A., Simpson, A. L., Adams, L. B., Jarnagin, W. R., and Miga, M. I., "Evaluation of model-based deformation correction in image-guided liver surgery via tracked intraoperative ultrasound," J. Med. Imaging (Bellingham), **3**, No. 1, 015003-1-015003-10 (2016).
42. Marinetto, E., Uneri, A., De Silva, T., Reaungamornrat, S., Zbijewski, W., Sisniega, A., Vogt, S., Kleinszig, G., Pascau, J., and Siewerdsen, J. H., "Integration of free-hand 3D ultrasound and mobile C-arm cone-beam CT: Feasibility and characterization for real-time guidance of needle insertion," Comput. Med. Imaging. Graph., **58**, 13-22 (2017).
43. Leonov, D. V., Kulberg, N. S., Gromov, A. I., Morozov, S. P., and Kim, S. Yu., " Causes of ultrasound Doppler twinkling artifact," Acoust. Phys., **64**, No. 1, 105-114 (2018).
44. Kulberg, N. S., Gromov, A. I., Leonov, D. V., Osipov, L. V., Usanov, M. S., and Morozov, S. P., "Ultrasound diagnostic mode for kidney stones and soft tissue calculi detection," Radiol.-Prakt., **67**, No. 1, 37-49 (2018).
45. Leonov, D., Kulberg, N., Gromov, A., Fin, V., Usanov, M., Kovbas, V., Sergunova, K., Strelkov, N., Vladzimirskiy, A., and Morozov, S., "Ultrasound stone detection: Discovery and analysis of two stone-related components in reflected signal and their role in etiology of twinkling artifact," Int. J. Comput. Assist. Radiol. Surg., **13**, Supplement 1, 10-11 (2018).
46. Leonov, D. V., Kulberg, N. S., Gromov, A. I., Morozov S. P., and Vladzimirskiy, A. V., "Diagnostic mode detecting solid mineral inclusions in medical ultrasound imaging," Acoust. Phys., **64,** No. 5, 624-636 (2018).
47. Tsujimoto, F., "Microcalcifications in the breast detected by a color Doppler method using twinkling artifacts: some important discussions based on clinical cases and experiments with a new ultrasound modality called multidetector-ultrasonography," J. Med. Ultrasonics, **41**, No. 1, 99-108 (2014).